Coral Reefs (2012) 31:425–439
DOI 10.1007/s00338-011-0860-1

REPORT

Detecting coral bleaching using high-resolution satellite data analysis and 2-dimensional thermal model simulation in the Ishigaki fringing reef, Japan

A. P. Dadhich · K. Nadaoka · T. Yamamoto · H. Kayanne

Received: 14 February 2011 / Accepted: 30 November 2011 / Published online: 24 December 2011

Abstract In 2007, high-temperature-induced mass coral mortality was observed in a well-developed fringing reef area on the southeastern coast of Ishigaki Island, Japan. To analyze the response of the corals to thermal stress, the coral cover was examined using Quickbird data, taken across the reef flat just before and after the bleaching event and performing a reef scale horizontal 2-dimensional thermal model simulation. The Quickbird data consisted of multispectral (MSS) imagery, which had a spatial resolution of 2.4 m, and panchromatic (PAN)-fused multispectral imagery, which had a 0.6-m spatial resolution. The observed changes in coral cover implied that the delineation of partially bleached coral was more precise with PAN + MSS. The classification accuracy achieved using PAN + MSS (93%) was superior to that obtained using MSS (88%). The in situ water temperature observations and 2-dimensional thermal model simulation results indicated that the water temperature fluctuated greatly in the inner reef area in late July 2007. Different thermal stress indices, including daily average temperature, daily maximum excess temperature, and daily accumulated temperature, were examined to define a suitable index that represented the severity of the thermal stress on coral cover. The results suggested that the daily accumulated temperature that occurred during the maximum sea surface temperature period of the bleaching season provided the best predictor of bleaching. The changes in water temperature, bathymetry, and coral patch size affected the severity of bleaching; therefore, the spatial dependence of these variables was examined using Moran's I and Lagrange multiplier tests. An investigation of the effect of coral patch sizes on coral bleaching indicated that large coral patches were less affected than the small patches, which were more likely to suffer bleaching and coral mortality.

Keywords Coral bleaching · Remote sensing · Quickbird · 2D thermal model · Spatial dependence

Communicated by Environment Editor Prof. Rob van Woesik

A. P. Dadhich (✉) · K. Nadaoka · T. Yamamoto
W8-13 Nadaoka Laboratory, Department of Mechanical and Environmental Informatics, Tokyo Institute of Technology, 2-12-1 O-okayama, Meguro-ku, Tokyo 152-8552, Japan
e-mail: ankita.d.aa@m.titech.ac.jp

H. Kayanne
Department of Earth and Planetary Science, University of Tokyo, Hongo, Tokyo 113-0033, Japan

Introduction

Coral reefs are considered to be among the most biologically diverse ecosystems on earth. They cover less than 0.2% of the ocean floor but contain approximately 25% of the ocean's species (Roberts 2003). They have much higher gross primary productivity than the surrounding ocean (Odum 1963; Weber 1993; IPCC 2007). These marine habitats have been significantly degraded and destroyed by human disturbances (Hughes 1994) and by natural anomalies that produce high sea surface temperatures, such as global warming (Hoegh-Gulberg 1999; Wellington et al. 2001; Douglas 2003; Gardner et al. 2003). Thus, the information on the status of coral reefs is crucial for their conservation and sustainable utilization. Corals are dependent upon specific conditions of temperature, light, salinity, turbidity and oxygen availability. When these environmental conditions are altered, the stress placed on the coral often causes bleaching because of (1) the decline in the densities of zooxanthellae and/or (2) the decreasing

concentrations of the photosynthetic pigments within the zooxanthellae (Kleppel et al. 1989). Although many factors are responsible for coral mortality, bleaching is viewed as the most important causal factor in both the widespread mortality of corals and changes in coral-reef community structures (Bruno et al. 2001; Diaz-Pulido and McCook 2002). Several mass-bleaching events have been recorded on coral reefs around the world during the last 25 years. There is concern that such events may be increasing in frequency (Brown 1997; Hoegh-Gulberg 1999; Sheppard 2003). Large-scale bleaching is triggered by elevated sea surface temperatures. Unprecedented increases in sea surface temperatures have occurred in many areas of the tropical oceans (Goreau et al. 2000; Loya et al. 2001; McClanahan 2004; McWilliams et al. 2005). During 1997–1998, severe coral bleaching was reported in many coral reefs in the tropical and subtropical regions of the world. Ishigaki Island, in southwest Japan, was also affected by this thermal event during 1998, and most of the *Acropora* species have disappeared from the island (Fujioka 1999; Hasegawa et al. 1999; Kayanne et al. 1999). Significant coral bleaching was observed on Ishigaki Island in late July 2007.

The field sampling approach for monitoring the coral-reef environments requires a large number of transect data and can therefore be costly and labor intensive. However, combining field information with remote sensing (Lee et al. 2003) offers an effective, complementary approach that can overcome the limitations of field sampling, particularly for the monitoring of reefs in remote areas. The loss of pigmented zooxanthellae from corals during bleaching events results in an optical signal that is strong enough to detect remotely. Most coral bleaching studies have suggested that it is difficult for satellite sensors to detect coral bleaching, primarily when the spatial resolution is low relative to the scale of reef heterogeneity (Holden and LeDrew 1998). A study of the 1998 bleaching event showed that information on bleached corals could be obtained using sensors with high (<2 m) spatial resolution (Andréfouët et al. 2002). Bleached corals have a high reflectance in blue-green spectral bands. This property enables the detection of a bleaching event. Holden and LeDrew (1998) and Clark et al. (2000) acquired high-resolution reflectance spectra of corals and found that bleached corals were approximately 10% brighter in the visible spectrum than healthy corals.

In this study, Quickbird data were used to investigate the coral assemblages affected by bleaching on the southeastern coast of Ishigaki Island. Quickbird was chosen because of its high spatial resolution (multispectral 2.4 m and panchromatic 0.6 m). The main objectives of this study were to map the severity of bleaching using multispectral (MSS) and panchromatic-fused multispectral (PAN + MSS) images of Quickbird, taken just before and just after the bleaching event in 2007, and to examine the spatial relationships between water temperature and bleaching. A comparison of images of before and during a bleaching event allows an accurate assessment of bleached and partially bleached corals. Different thermal stress indices were also developed to define a suitable index that would represent the effects of thermal stress on coral cover. The selected thermal stress index was designed to take into account spatio-temporal variations in the inner reef area using a reef scale 2-dimensional thermal model. We also sought to evaluate the spatial dependence of the damaged coral cover on changes in bathymetry, water temperature and coral patch size (delineated using Quickbird imagery) based on MSS and PAN + MSS images.

Methods

Study area

Ishigaki Island is situated near the southern end of the Ryukyu Islands of Japan (24°23′N latitude, 124°14′E longitude), 430 km southwest of the main island of Okinawa (Fig. 1a). Ishigaki Island is almost completely surrounded by well-developed fringing reefs, 0.5–1.4 km wide. Four channels, named Tooru-guchi, Ika-guchi, Moriyama-guchi, and Bu-guchi, exist on the southeastern coast of Ishigaki (Fig. 1c). Tooru-guchi, the largest channel, penetrates deeply into the reef and has an average depth of 20 m (Tamura et al. 2007). The climate of Ishigaki is subtropical. The annual mean temperature is 24.3°C, the annual mean relative humidity is 78%, and the annual mean precipitation is approximately 2,000 mm. Two rainy seasons occur annually (1) the monsoon season (from March to May) and (2) the typhoon season (from July to September). The dominant wind direction is southerly in summer and northerly in winter. The reef supports a dense population of the blue coral *Heliopora coerulea*. This population is considered to contain the oldest and largest known colonies of this coral in the world (Planck et al. 1988).

Image acquisition and preprocessing

The Quickbird images (image acquisition dates June 27 and September 25, 2007) were taken just before and just after the peak of bleaching event in 2007 with full 16-bit radiometric resolution and spatial resolutions of 2.4 m (MSS) and 0.6 m (PAN) to quantify coral bleaching in the study area. The image subsets from the Quickbird panchromatic (3,922 width × 16,212 height) and multispectral sensors (982 width × 4,055 height) covering a portion of the southeastern coast of the Ishigaki reef area were prepared for further processing. In image preprocessing, the image was radiometrically calibrated to retrieve at-sensor radiance and then

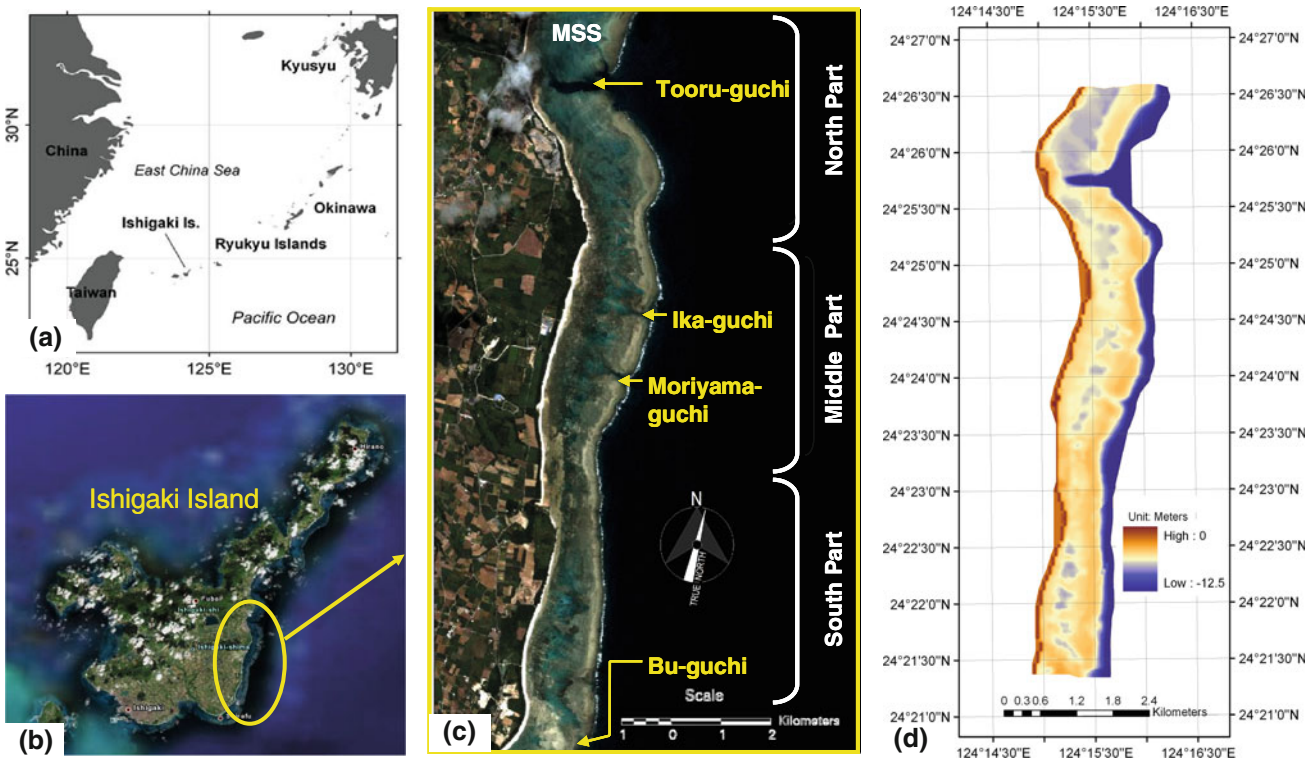

Fig. 1 Study site **a** location of Ishigaki Island; **b** southeastern coast of Ishigaki Island; **c** Quickbird image (multispectral) of the southeastern coast of Ishigaki; **d** bathymetric map of the study area

atmospherically corrected using the Fast Line-of-Site Atmospheric Analysis of Spectral Hypercubes (FLAASH) atmospheric correction module of the ENVI image processing software package (http://www.RSInc.com/envi). FLAASH incorporates MODerate spectral resolution atmospheric TRANsmittance algorithm (MODTRAN4) radiative transfer code (Matthew et al. 2000). In addition to the corrections for atmospheric absorption and scattering, FLAASH model corrects for adjacency effects (i.e., pixel mixing due to scattering of surface-reflected radiance). A manually digitized land and deep-water mask was applied to focus the image processing on the shallow water of the southeastern coast of the Ishigaki Island. Thereafter, the water column correction was performed using the depth-invariant index proposed by Lyzenga (1981) to enhance the information on the bottom type. This concept is based on the assumption that bottom-reflected radiance is a linear function of the bottom reflectance and an exponential function of the water depth. To construct a linear relationship between the radiance and the depth, the radiance value, which has been atmospherically corrected, was transformed using the natural logarithm (ln). To generate a depth-invariant index of bottom types within a pair of bands, the following equation is used:

$$\text{Depth-invariant index}_{ij} = \ln(L_i) - \left[\left(\frac{k_i}{k_j}\right) \times \ln(L_j)\right] \quad (1)$$

where $\ln(L_i)$ = natural logarithm of a pixel in band i

$\ln(L_j)$ = natural logarithm of a pixel in band j

k_i/k_j = attenuation coefficient

Image classification

The water-column corrected images were enhanced by applying a texture filter (Andréfouët and Guzman 2005; Franklin et al. 2003) to improve the visibility and detectability of different benthic features and classified as coral, algae, seagrass, pavement, sand and rubble using a maximum likelihood decision rule. For defining the decision rule, training samples were selected for each of the benthic cover types to perform the supervised classification. The training samples were created using georeferenced photo transects, spot checks and local expert knowledge. Each training sample consisted of at least 90 image pixels to satisfy the $10n$ criteria. The parameter n refers to the number of bands used for classification (Congalton 1991). A few misclassified image pixels were reassigned manually to the correct classes based on local knowledge and the Quickbird image. From this classified output, the areas identified as coral were masked out and overlaid over the original image to further reclassify the coral cover visually as live coral, partially bleached coral (i.e., a portion bleached, with some live coral tissue), fully bleached coral (i.e., 100% bleached with no algal

colonization) and dead coral (i.e., coral tissue areas partially overgrown by an algal turf layer). For the identification of coral cover, the coral location, color and texture were used for better interpretation. Band 1 (0.45–0.52 μm) and Band 2 (0.52–0.60 μm) of the Quickbird data were used to identify the fully bleached coral pixels (Elvidge et al. 2004). The coral cover patches were delineated visually over the image on the basis of the homogeneous shape and texture for spatial dependence analysis.

These classified coral classes were then confirmed at seven locations (Table 1) using ground-truthed data along five fixed transect lines (N12, N06, CL, S06 and S12) of the study area. The accuracy assessment was performed by comparing the classified output with the satellite image and ground truth locations using Erdas Imagine 9.3, an Image analysis software of Leica Geosystems Geospatial Imaging (http://www.erdas.com). The overall accuracy, along with kappa statistics, was used to determine the precision of thematic map in order to examine whether any difference exists in the image interpretation. Kappa statistics determine overall accuracy of image classification and individual class accuracy as a means of actual conformity between classification and observation. The value of Kappa lies between 0 and 1, where 1 represents complete agreement between the classified data and reference data. The classification results were then exported to a Geographic Information System (GIS) for further analysis.

Spatio-temporal dynamics of coral bleaching

Temperature and bathymetry data

The spatial and temporal variations in the water temperature across the reef were simulated based on the horizontal 2-dimensional reef thermal transport model of Tamura and Nadaoka (2005). The input parameters used for the temperature simulation included the results of a hydrodynamic simulation based on the model proposed by Tamura et al. (2007). Other input parameters included observations of the wind velocity, air temperature, vapor pressure and atmospheric pressure collected by the Japan Meteorological Agency at the Ishigaki Meteorological Observatory. The in situ measurements of surface and bottom water temperature were taken in the study area during May 16 to September 27, 2007, using Hobo Water Temperature Pro data loggers. The in situ observations indicated a rise in the water temperature in late July. Therefore, we performed a temperature simulation for late July 2007. Figure 2a indicates the locations where we deployed in situ loggers in the inner and outer reef areas and recorded water temperature at 10-min intervals. The meteorological conditions are shown in Fig. 2b. The detailed temporal variations in the inner reef area and outer reef area are represented in Fig. 2c for the southern part of the southeast coast of Ishigaki Island. The water temperatures began increasing on July 17, 2007; so, the temperature simulation computations were performed for the period from July 17 to 27, 2007, to

Table 1 Details of coral bleaching survey

Location with distance from coast	Latitude/ longitude	Survey period	Coverage (%)	Dominant species with percentage	Condition (%)			
					L	PB	FB	D
① N12 (50–200 m)	N24°22′10.7″ E124°15′07.1″	10/1/2007	5	Massive porites (5)	40	0	15	45
② N12 (500 m)	N24°22′51.5″ E124°15′19.1″	10/1/2007	5	Massive porites (3)	80	0	10	10
				Pavona (2)	45	0	0	55
③ N6 (650–700 m)	N24°22′01.1″ E124°15′23.3″	10/1/2007	5	Massive porites (5)	75	0	10	15
④ CL (100–150 m)	N24°21′51.5″ E124°15′01.6″	10/2/2007	5	Massive porites (5)	30	0	30	40
⑤ CL (550–600 m)	N24°21′51.7″ E124°15′17.4″	10/2/2007	30	Branching porites (20)	95	5	0	0
				Heliopora coerulea (10)	95	5	0	0
⑥ S6 (500 m)	N24°21′41.6″ E124°15′16.1″	10/1/2007	10	Heliopora coerulea (10)	95	5	0	0
⑦ S12 (700 m)	N24°21′32.1″ E124°15′19.7″	10/1/2007	5	Heliopora coerulea (5)	95	5	0	0

L live, *PB* partially bleached, *FB* fully bleached, *D* dead

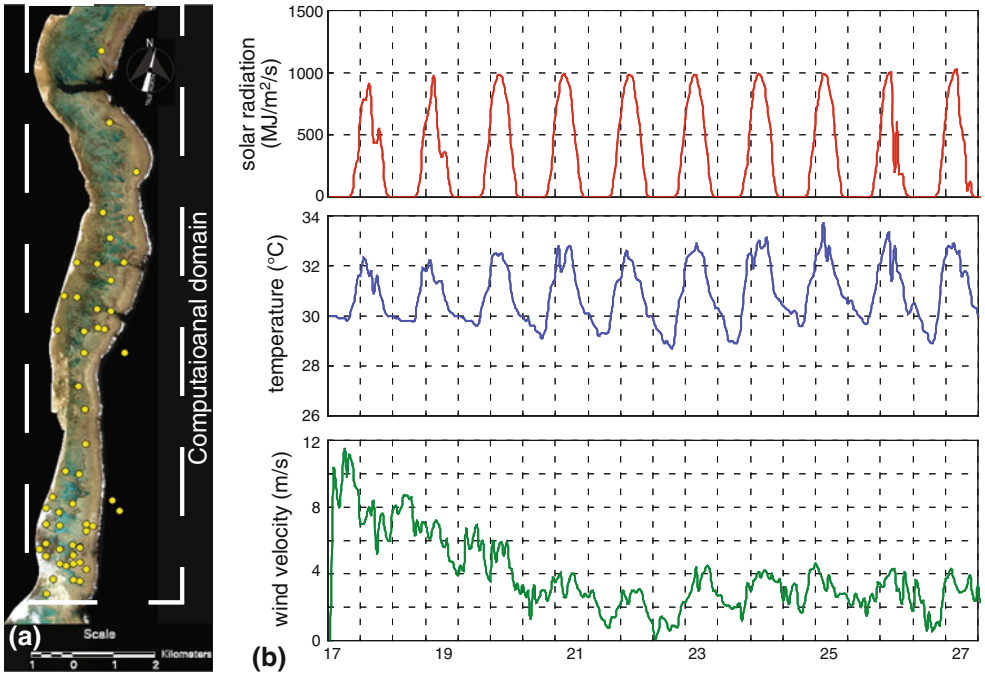

Fig. 2 **a** The Quickbird image of the southeastern coast of Ishigaki Island indicating the locations (*yellow dots*) in the inner and outer reef area where the in situ loggers were deployed and the computational domain for the temperature simulation; **b** meteorological conditions in late July 2007. **c** temporal variation at different locations in the study area and validation of the simulated temperature in the inner reef area from July 21 to 26, 2007

provide a detailed and quantitative understanding of the spatiotemporal variation in the fringing coral reefs. The temperature simulation results were later converted to grid format for further analysis in GIS.

In this study, we used bathymetric data created by Paringit and Nadaoka (2003). These authors employed remotely sensed multispectral imagery (IKONOS) and nautical charts. The depth values were plotted for each coral patch in Geographic Information System (GIS). GIS was used to create a database of the thermal stress indices calculations, spatial dependence analysis and the patch size distribution.

Temperature simulation analysis

For the data analysis, the simulation region was divided into three parts (north, middle and south), as indicated in Fig. 1. The sea-water temperature data recorded between July 21 and 26, 2007, were used to validate the temperature simulation results (Fig. 2c). The temporal resolution of the temperature simulation was 15-min and the in situ observations were recorded at 10-min intervals; therefore, we validated the temperature simulation results with the observed data at 30-min intervals. The temperature simulation results were validated near the coast (H02), in the moat area (ST6 and ST13), in the coral cover area (ST10-1) and at the reef crest (ST2).

Many research studies include Degree Heating Weeks (DHW) as a measure of thermal stress and calculate DHW using monthly time-scale datasets, which is used to derive regional synoptic assessments. In this study, we examined thermal stress indices at the local reef scale. We used short time-scale (15-min interval) datasets to understand the dynamics of the change in the water temperature. We examined three thermal stress indices to identify which would be the best predictor of bleaching. These three thermal indices were examined in GIS using the simulation results to enable selection of a suitable index for representing the severity of the thermal stress on coral cover.

Calculation of thermal stress indices

The water temperatures across and outside the reef area (the computational domain is shown in Fig. 2a) were simulated based on the reef thermal transport model of Tamura and Nadaoka (2005). For each 50 by 50 m grid, the simulation results were analyzed in Excel spreadsheets to calculate the daily average temperature, the daily maximum excess temperature and the daily accumulated temperature. A schematic diagram of the method used to calculate these indices is shown in Fig. 3. The calculated values of each index were categorized into different temperature regimes to improve interpretation of the results. In the first index, the daily average temperature was

Fig. 2 continued

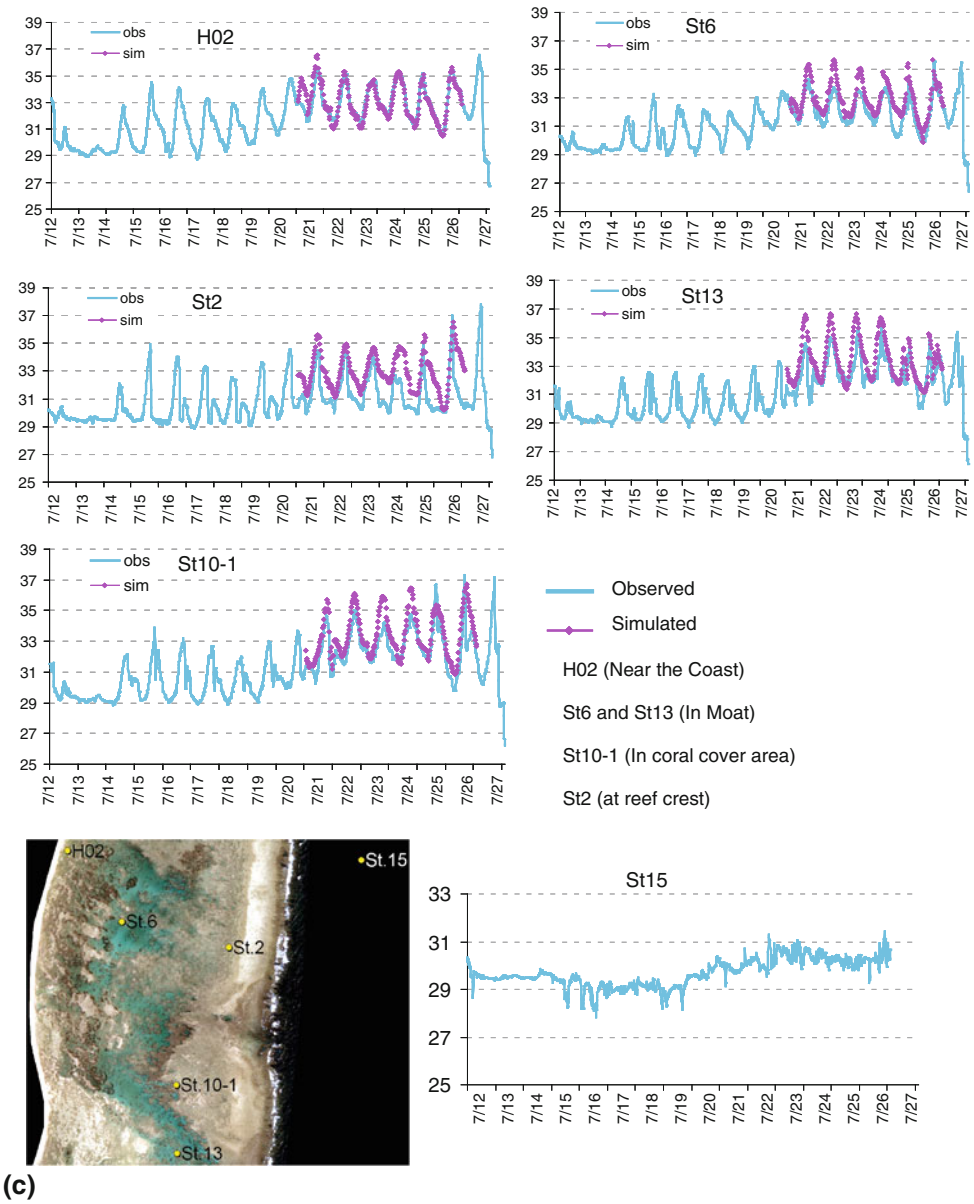

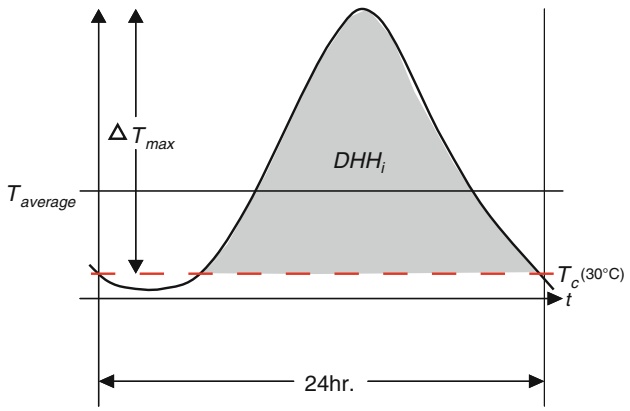

Fig. 3 Schematic diagram for the calculation of the different thermal stress indices

considered by defining four temperature ranges: ≤31°C, 31–31.5°C, 31.5–32°C and ≥32°C. The second index is defined by the daily maximum excess temperature using the following expression:

$$\Delta T \max_i = T \max_i - T_c \quad (2)$$

where $\Delta T\,\max_i$ is the daily maximum excess temperature at the ith location

$T\max_i$ is the daily maximum temperature at the ith location

T_c is a critical temperature, assumed to have the value 30°C

To calculate the daily maximum excess temperature, the daily maximum temperature was considered at each coral

location at 15-min intervals. The critical water temperature of 30°C was used because bleaching was observed in the study area in 1998 when the SST exceeded 30°C (Kayanne et al. 1999). Four regimes of daily maximum excess temperature were defined: ≤2°C, 2–4°C, 4.1–6°C and >6°C. These categories were used to examine the impact of increased water temperature on coral cover. The third index included the daily accumulated temperature, or Degree Heating Hour (DHH_i), which was calculated as the accumulated amount of heat according to the following equation:

$$\mathrm{DHH}_i = \int_{t \subset t*} (T_i - T_c)\mathrm{d}t \cong \sum_{t \subset t*} (T_i - T_c)\Delta t \quad (3)$$

where DHH_i is the cumulative temperature for 1 day (specifically, the sum of the positive deviations)

T_i is the temperature at the ith location, using 15-min intervals
T_c is a critical temperature, assumed to be 30°C
$t \subset t*$ is the time period where $T_i > T_c$
Δt is the time increment between the discretized temperature data.

Five groups of DHH_i values were defined: ≤6°Chr, 6–10°Chr, 10.1–14°Chr, 14.1–18°Chr and >18°Chr. Later, these daily average temperatures, daily maximum excess temperatures and daily accumulated temperature DHH_i values were converted into a grid format for further GIS analysis of the effects of thermal stress on coral cover. To calculate the stress on each coral cover category, we overlaid the coral cover thematic layer on these different temperature grids. Using the query generate option in GIS, we then identified the coral-covered areas within each zone of each index. The areas covered by partially bleached, fully bleached and dead corals were then correlated with the temperature regimes to discover which index best represented the severity of the thermal stress.

Spatial dependence analysis

Spatial dependence analysis indicates the dependence of different variables and their spatial autocorrelation. Here we hypothesized that changes in water temperature, bathymetry and coral patch size affected coral cover. Therefore, for this analysis, the coral cover was used as the dependent variable whereas water temperature, bathymetry and patch size were used as the independent variables. To understand the spatial dependence of these variables, multivariate Moran's I was calculated (Moran 1950). The possible values of this index range between −1.0 and +1.0. Briefly, −1 indicates strong negative spatial autocorrelation (i.e., a checkerboard pattern), 0 indicates random spatial ordering and +1 indicates strong positive spatial autocorrelation (i.e., clustering of similar values). Moran's I was calculated using the following equation:

$$I = \frac{N \sum_i \sum_j W_{i,j}(X_i - \bar{X})(X_j - \bar{X})}{\left(\sum_i \sum_j W_{i,j}\right) \sum_i (X_i - \bar{X})^2} \quad (4)$$

where N is the number of cases

X_i is the variable value at a particular location
X_j is the variable value at another location
$\bar{X}$ is the mean of the variable
$W_{i,j}$ is a weight applied to the comparison between location i and location j

The Lagrange multiplier (LM) test is a general principle for testing hypotheses about parameters in a likelihood framework. The hypothesis under test is expressed as one or more constraints on the values of parameters. To perform the LM test, the only estimation of the parameters subject to the restrictions is required. Any spatial data may show spatial dependence of the variables in the lag and error terms, therefore we used the testing procedure of Anselin (2005) to conduct Lagrange multiplier tests for spatial lag and spatial error dependence.

Results

Coral cover change with PAN + MSS and MSS

Image interpretation indicated that the total area covered by corals identified from the PAN + MSS image (24.9 ha) was larger than that identified from the MSS image (21.17 ha). The accuracy of the September 2007 image-classified output was assessed using an error matrix. This accuracy assessment was performed by comparing the classified output with the satellite image and the ground truth locations using the Image analysis software. For this purpose, the accuracy of the first classification output of the September image was checked with the satellite data for the coral, algae, seagrass, pavement, and sand and rubble classes by generating random points throughout the study area to assess the quality of the classified output. The overall accuracy for the benthic cover classification was 87.39% for MSS and 91.74% for PAN + MSS. In the next step, the accuracy was assessed for the coral classes (live, partially bleached, fully bleached and dead) using ground truth data collected on October 1 to 2, 2007, at seven locations along five fixed transect lines. The overall accuracy values for the corals classes were 88.25% (MSS) and 92.59% (PAN + MSS), respectively, whereas the kappa indices for MSS and PAN + MSS were 0.87 and 0.93, respectively. Figure 4 and Table 2 represent the coral

cover area on September 25, 2007, with the coral classified into four different categories, namely live coral, partially bleached coral, fully bleached coral and dead coral. Table 2 shows that 88.14% (MSS) and 77.85% (PAN + MSS) of the total coral cover was affected by bleaching. The coral cover interpretation (Table 2) indicated that 60.7% of the corals were partially bleached, 22.72% were fully bleached and 4.72% were dead according to the MSS results. The PAN +MSS results showed 61.79% partially bleached, 11.86% fully bleached and 4.2% dead. It is clear from Table 2 that the proportions of healthy coral and partially bleached coral cover were higher in the PAN + MSS data, the fully bleached coral cover in the PAN + MSS data was lower in comparison with the MSS data, and the dead coral cover was almost the same in both of the images (MSS and PAN + MSS).

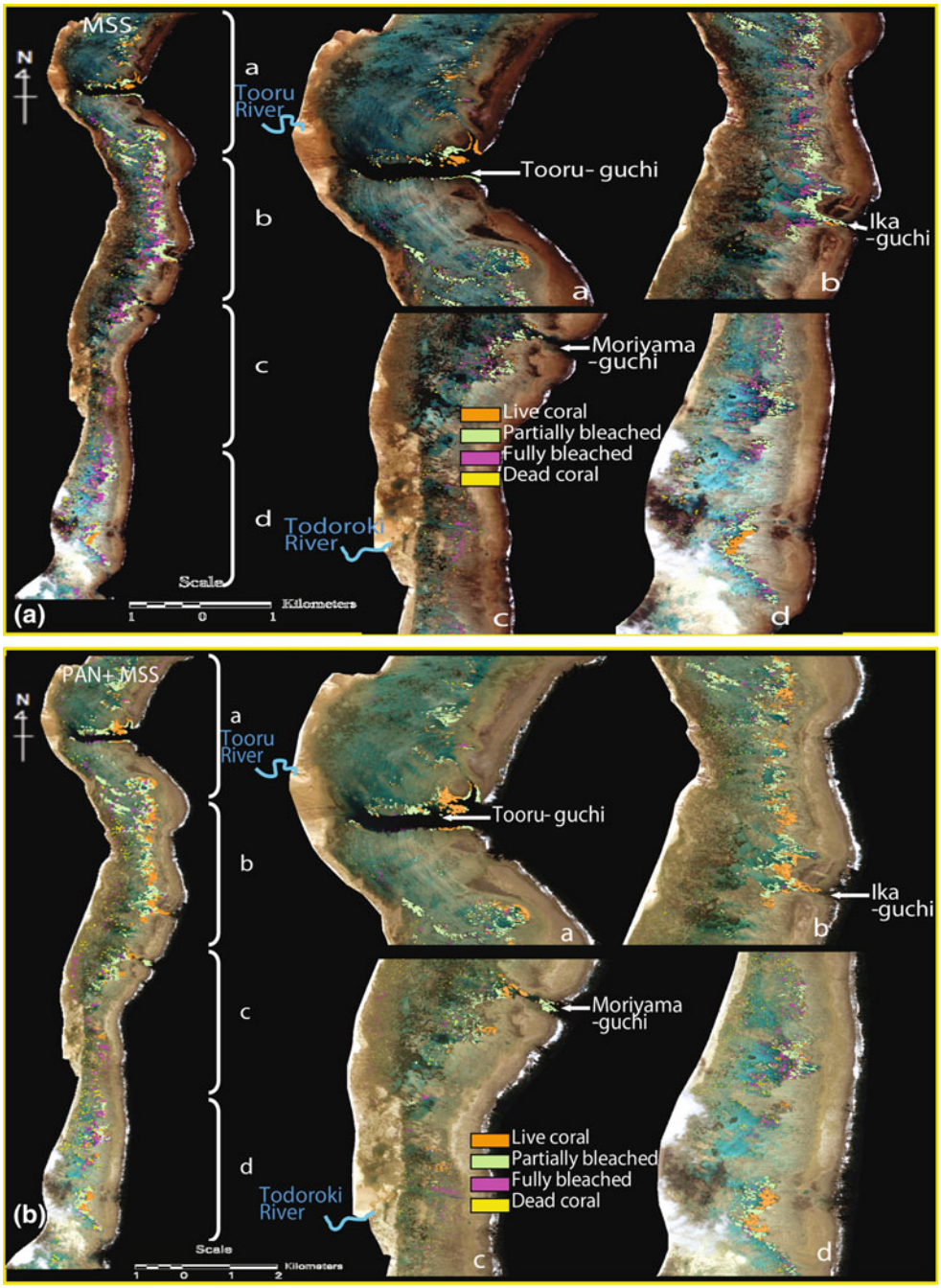

Fig. 4 Coral cover in September 2007 using **a** MSS data and **b** PAN + MSS data

Table 2 Coral cover change from June to September 2007 for MSS and PAN + MSS data

June 2007	September 2007	Coral cover change			
		MSS		PAN + MSS	
		Area (ha.)	Area (%)	Area (ha.)	Area (%)
Live coral	Live coral	2.51	11.86	5.52	22.15
Live coral	Partially bleached	12.85	60.70	15.39	61.79
Live coral	Fully bleached	4.81	22.72	2.95	11.86
Live coral	Dead coral	1.00	4.72	1.04	4.20
Sub-total of damaged corals		18.66	88.14	19.38	77.85
Total		21.17	100	24.9	100

Spatial and temporal distribution of corals

The in situ temperature measurements (Fig. 2c) showed that more abrupt changes in water temperature occurred at locations ST2 and ST13, close to the reef crest. The overall water temperature increase on the reef was augmented by an atmospheric effect in late July, because the wind strength became so weak that the latent heat flux to the air decreased. The temperature simulation results closely matched the observed values at all of the locations. The standard error between observed and simulated data was 0.54 (near the coast, at location H02), 0.57 and 0.81 in the moat area (location ST6 and ST13), 0.69 in the coral cover area (location ST10-1) and 0.88 at the reef crest (location ST2). The temperature simulation results (Fig. 5a) demonstrated the variation in the spatial distribution of daily mean sea-water temperature from July 21 to 26, 2007. Similarly, the in situ results indicated that the daily mean temperature outside of the reef was approximately 29°C until 20 July and increased to 30.5°C in late July (Fig. 2c). Whereas in the inner reef area, the daily mean temperature increased to 33°C in late July, and the daily minimum temperature exceeded 30°C from 21 July onwards. The simulated water temperature averaged every 4 h on 26 July (Fig. 5b) showed that the temperature remained relatively higher in the middle and southern parts of the study area. The simulation results showed rapid temperature rise on July 26, 2007, and an increase in the maximum average temperature to 37.6°C between 12:30 and 16:30 h near the coast and at the reef crest.

The temperature simulation results showed that the maximum daily mean temperature was on July 26, 2007, in our study area. Therefore, we focused on the temperature simulation results of July 26, 2007, at 15-min intervals to calculate the thermal stress indices because bleaching can be induced by short-term exposure (1–2 days) to high temperatures (Jokiel and Coles 1990). Figure 6 displays the spatial distribution of all the three thermal indices with different water temperature regimes on July 26, 2007. The GIS analysis results indicated that partially bleached and dead corals were not well correlated with the daily average temperature index for MSS and PAN + MSS. However, the fully bleached corals increased and the live coral decreased with the rise in water temperature (Fig. 7a, Table 3). The results for daily maximum excess temperature indicated that none of the damaged coral categories (partially, fully bleached and dead corals) were well correlated with the daily maximum excess temperature ranges (Fig. 7b, Table 4). As the daily accumulated temperature index increased, the live corals and the partially bleached corals showed decreasing trends for both the MSS and the PAN + MSS data, whereas the fully bleached corals and dead corals increased with increasing daily accumulated temperature (Fig. 7c, Table 5). The correlation (r^2) between the bleaching severity and the thermal stress was highest for the daily accumulated temperature (0.81 MSS, 0.85 PAN + MSS), had intermediate values for the daily average temperature (0.63 MSS, 0.71 PAN + MSS) and was lowest for the daily maximum excess temperature (0.61 MSS, 0.68 PAN + MSS). The results for these three thermal stress indices indicate that the bleaching severity could be best interpreted in terms of the daily accumulated temperature occurring during the maximum SST period of the bleaching season.

Spatial dependence of variables

The changes in water temperature, bathymetry and coral patch size may affect the severity of the bleaching. Therefore, to evaluate the spatial dependence of different variables such as water temperature, bathymetry and coral patch size with respect to the damaged coral cover, these layers were overlaid on coral cover in GIS. A spatial dependence analysis using Moran's I and Lagrange multipliers on both the error and lag terms showed that water temperature, bathymetry and patch size had direct effects on coral cover. The Moran's I scores of 0.3965 (MSS) and 0.4251 (PAN + MSS) were highly significant and

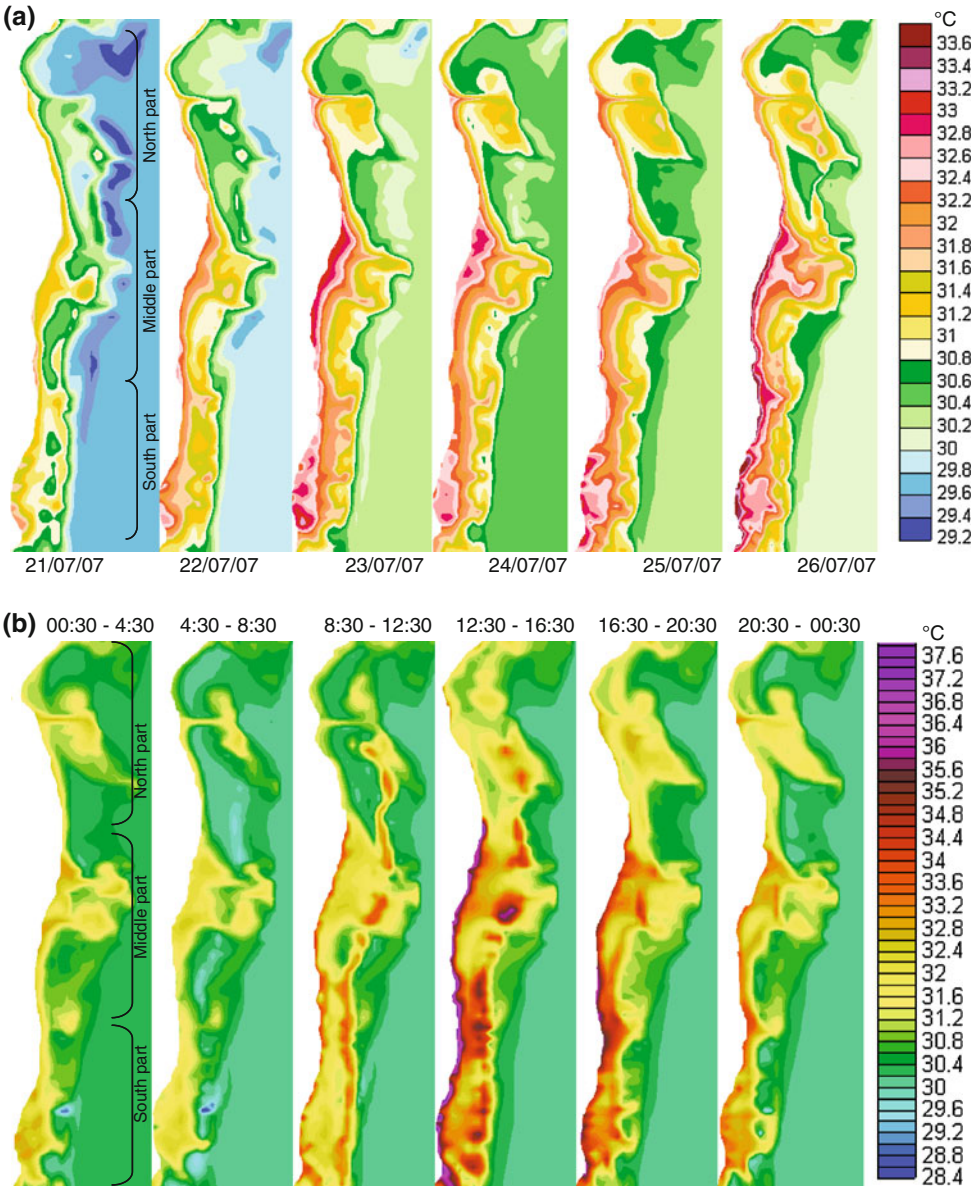

Fig. 5 **a** Spatial distribution of the daily average water temperature from July 21 to 26, 2007; **b** spatial distribution of water temperature averaged every 4 h on July 26, 2007

indicated strong spatial autocorrelation of the residuals. We also calculated the Moran's *I* independently for each of the variables. The values obtained for PAN + MSS were 0.1884 (temperature) and 0.1836 (depth). These values were slightly greater than those found for MSS (Moran's $I = 0.0756$ and 0.1583, respectively). Patch size showed less positive autocorrelation with the residuals than did temperature and bathymetry. The autocorrelation for patch size was greater for PAN + MSS (Moran's $I = 0.094$) than for MSS (Moran's $I = 0.0432$). The Lagrange multiplier (lag) and Lagrange multiplier (error) had highly significant positive values, 1,569.35 ($P < 0.00$) and 1,486.82 ($P < 0.00$) for the MSS data and 4,011.36 ($P < 0.00$) and 3,660.26 ($P < 0.00$) for the PAN + MSS data, respectively. The results from the spatial lag model and the spatial error model indicated the presence of spatial dependence. The PAN + MSS data show more spatial dependence of the variables compared with the MSS data.

Coral patch size distribution

The coral recovery response in the 2-year period following bleaching has been shown to vary according to patch size (Kayanne et al. 2002). Therefore, patch size not only affects the short-term bleaching response to thermal stress but also affects the capacity to recover. To investigate the thermal stress effect on different coral patch sizes using the MSS and PAN + MSS images from Quickbird, the coral patches were categorized into five classes (≤10, 10–30, 30.1–60, 60.1–90, and ≥90 m^2) based on the area of the

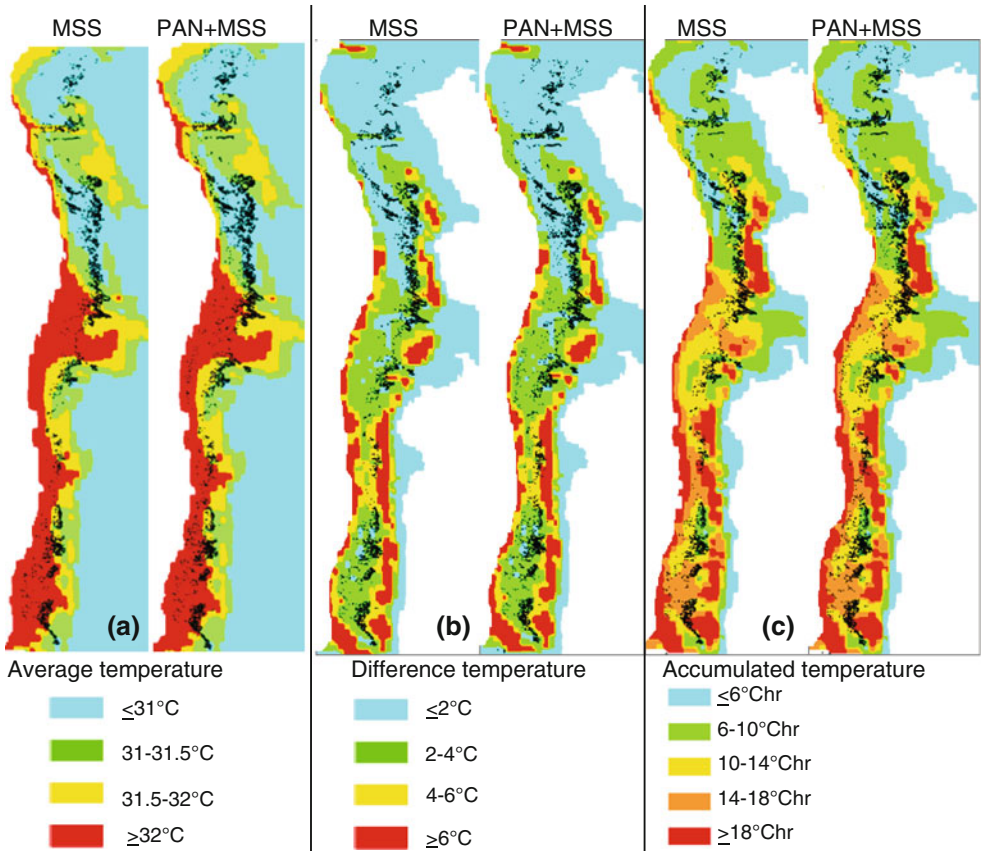

Fig. 6 Spatial distribution of thermal indices with different water temperature regimes on July 26, 2007. *Remarks*: *black color* denotes the coral cover

patches. The histograms of coral patch sizes (Fig. 8) show that the fully bleached and dead corals most frequently occupied areas ≤10 m^2. The MSS data showed no live or a partially bleached coral class for ≤10 m^2 areas. In the 10–30 m^2 area category, the fully bleached corals dominated (57.6%) in the MSS data, and the partially bleached (36.9%) and fully bleached (39.4%) corals showed dominance in the PAN + MSS data. For the 30.1–60 m^2 area category, the MSS and PAN + MSS data indicated that the fully bleached corals and partially bleached corals represented 58.9 and 55.96% of the total, respectively. In the 60.1–90 m^2 category, the PAN + MSS data exhibited a maximum percentage of partially bleached corals (66.1%). However, the fully bleached corals (48.6%) dominated this area category in the MSS data. In the ≥90 m^2 area category, the MSS and PAN + MSS data indicated the dominance of the partially bleached and live corals. These results indicated that coral patches with area ≤10 m^2 were more susceptible to bleaching. Most of the corals in this category were either fully bleached or dead. The superior delineation of the smaller patches using the PAN + MSS data is noteworthy. Indeed, no live or partially bleached coral cover was found in the ≤10 m^2 category in MSS (Fig. 8). Findings from both images suggest that large coral patches were less affected by bleaching even at high temperatures, whereas small patches were more prone to bleaching even with only a slight rise in temperature.

Discussion

Mass coral bleaching is one of the most pressing issues affecting reef health. Identification of the causes of bleaching requires compilation of reef scale data on key disturbance factors. The primary goal of this study was to assess the utility of the higher spatial and radiometric resolution of the Quickbird data for mapping changes in coral cover and the detection of stress effects. Changes in the distribution of coral cover were tracked across the inner reef area by analyzing the Quickbird imagery. This study demonstrates enhanced mapping and monitoring capabilities for shallow-water benthic communities compared with the capabilities offered by Landsat TM and IKONOS. The studies conducted with Landsat TM data by Yamano and Tamura (2004) for Ishigaki Island were able to detect only 25–55% cover of the bleached corals on a reef flat, and

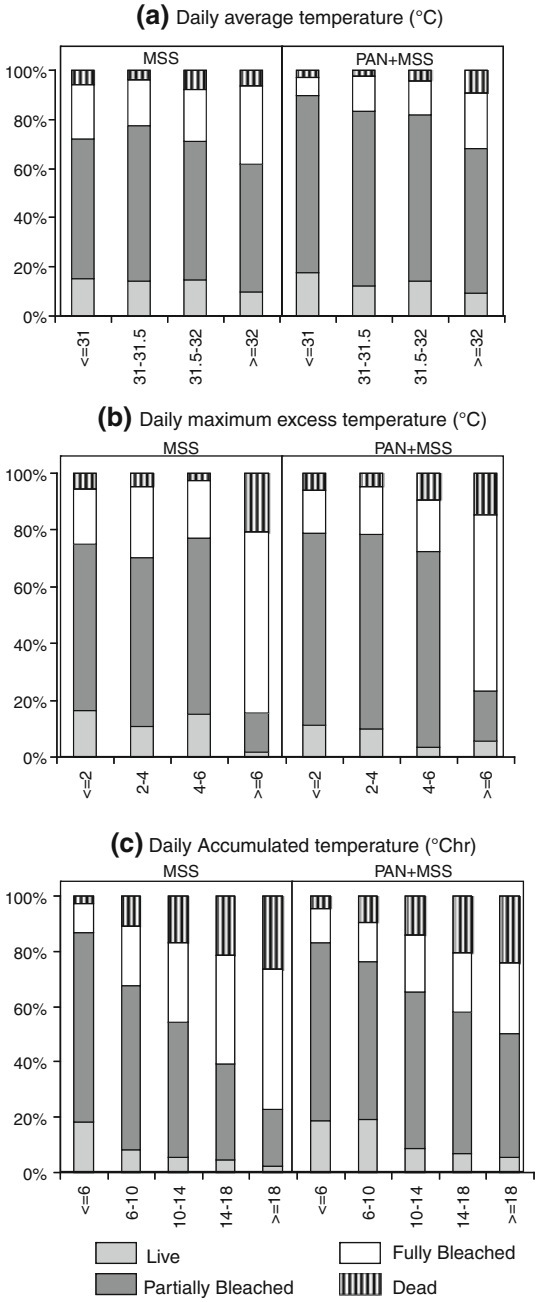

Fig. 7 Graphical representations of the different thermal stress indices indicating the severity of the stress on the coral with varying water temperature for July 26, 2007

partially bleached coral was difficult to detect owing to poor resolution. Andréfouët et al. (2002) suggested that monitoring and mapping of bleaching events remained unclear, even with 4 m (IKONOS) resolution and that the highest accuracy that could be obtained was in the 40–80 cm resolution range. Therefore, an examination of the Quickbird satellite imagery of the southeastern coast of Ishigaki Island acquired before and after a bleaching event indicated that the classification accuracy for bleached corals could be increased by using the Quickbird high spatial resolution data, especially PAN + MSS data. The pre-bleaching image served as a reference to accurately identify bleached or partially bleached corals (Elvidge et al. 2004). This research produced improved classification accuracy and accurate quantitative data on the severity of coral bleaching by using pre- and post-bleaching data from Quickbird. The comparative analysis of the PAN + MSS and MSS imagery indicated that PAN + MSS most clearly discriminated the spatial distribution of coral cover and offered improved detection of the severity of coral bleaching.

In this study, remote sensing data products were integrated in GIS with in situ observation data and numerical simulation results for analysis and application. The relationship of the changes in coral cover to the water temperature characteristics was investigated using in situ observation data and performing a horizontal 2-dimensional thermal model simulation at the reef scale. This simulation accurately represented the increase in the mean water temperature to 37.6°C during the daytime on July 26. The results of the bleaching analyses imply that the southern and middle parts of the reef were more affected by bleaching than the northern part of the reef. The temperature remained higher in the inshore areas in comparison with the offshore areas because of meteorological conditions and hydrodynamic processes. The thermal environment on the reef is influenced by atmospheric conditions and by temperature differences between the inside and outside of the reef (Nadaoka et al. 2001) caused by hydrodynamic processes. The in situ observations and temperature simulation results indicated that the northern part of the study area was least affected by bleaching because of the presence of the Tooru channel, a large channel that enhanced the water circulation between the inside and the outside of the reef.

Bleaching can be induced by short-term exposure (i.e., 1–2 days) to temperature elevations of 3–4°C above normal summer ambient values or by long-term exposure (i.e., several weeks) to elevations of 1–2°C (Jokiel and Coles 1990). We used short time-scale datasets to understand the dynamics of the change in the water temperature, and developed three thermal stress indices to identify the best predictor of bleaching. The results suggest that the relationship of thermal stress to coral bleaching is well represented by the daily accumulated temperature or DHH_i occurring during the maximum SST period, rather than by the daily average or the daily maximum excess temperature.

Analysis of the spatial dependence diagnostics suggested that the thermal conditions and bathymetry had significant impacts on coral mortality. However, patch size showed less positive autocorrelation with the residuals than

Table 3 Coral distribution in different temperature ranges (daily average temperature)

Coral class (area in %)	MSS (temperature ranges)				PAN + MSS (temperature ranges)			
	≤31	31–31.5	31.5–32	≥32	≤31	31–31.5	31.5–32	≥32
Daily average temperature								
Live	14.97	14.20	14.71	10.00	17.59	12.18	14.26	9.17
Partially bleached	57.07	63.25	56.3	51.80	72.22	70.99	67.42	58.73
Fully bleached	22.25	18.58	21.3	32.00	7.17	14.37	13.80	22.81
Dead	5.71	3.97	7.69	6.20	3.02	2.46	4.51	9.29
Total of damaged coral	85.03	85.80	85.29	90.00	82.41	87.82	85.74	90.83

Table 4 Coral distribution in different temperature regime (daily maximum excess temperature)

Coral class (area in %)	MSS (temperature ranges)				PAN + MSS (temperature ranges)			
	≤2	2–4	4–6	≥6	≤2	2–4	4–6	≥6
Daily maximum excess temperature								
Live	16.51	10.78	15.00	1.55	11.20	9.84	3.40	5.60
Partially bleached	58.53	59.50	62.00	14.00	67.63	68.64	69.21	17.81
Fully bleached	19.34	25.06	20.55	63.56	15.08	16.84	17.89	62.03
Dead	5.63	4.66	2.45	20.89	6.08	4.67	9.50	14.57
Total of damaged coral	83.49	89.22	85.00	98.45	88.80	90.16	96.60	94.40

Table 5 Coral distribution in different temperature regime (daily accumulated temperature)

Coral class (area in %)	MSS (temperature ranges)					PAN + MSS (temperature ranges)				
	≤6	6–10	10–14	14–18	≥18	≤6	6–10	10–14	14–18	≥18
Daily accumulated temperature										
Live	18.43	8.30	5.67	4.57	2.25	18.75	19.17	8.56	6.87	5.38
Partially bleached	68.34	59.28	48.56	34.83	20.60	64.46	57.03	56.66	50.93	44.74
Fully bleached	10.48	21.67	28.85	39.34	50.51	12.19	14.41	20.48	21.74	25.55
Dead	2.76	10.75	16.92	21.26	26.64	4.60	9.39	14.30	20.46	24.34
Total of damaged coral	81.57	91.70	94.33	95.43	97.75	81.25	80.83	91.44	93.13	94.62

did temperature and bathymetry. Indeed, the corals in deeper areas and large patches were less affected by bleaching. The higher tolerance to thermal stress of larger patches may result from the species-specific stress dependence of the corals. Loya et al. (2001) suggested that colony growth form and tissue thickness influence coral vulnerability. The dominant corals in the study area are *Heliopora coerulea*, massive *Porites*, branching *Porites*, *Montipora*, *Acropora* and *Pavona*. *H. coerulea* is the least susceptible to bleaching, whereas branching *Porites*, *Montipora* and *Acropora* are the most susceptible to bleaching (Kayanne et al. 2002). The health of the coral-reef ecosystem therefore depends on species composition as well as on patch size. The response of corals to thermal stress is species-specific and depends on the strategy that the corals use to resist bleaching. Unfortunately, the species distribution data for the study area were quite limited. Species distributions were available only for the southern part of the reef area. This limitation prevented species-dependent validation of the results. Examination of the species-specific tolerance to thermal stress therefore represents an important topic for future research.

Kayanne et al. (2002) reported that recovery of branching *Montipora*, 2 years after the mass coral bleaching of 1998 was correlated with patch size. They found that large patches recovered better than small patches. Therefore, it is expected that the occurrence of coral bleaching as a short-term response to thermal stress may also exhibit patch size dependence. The effect of coral patch size distribution was also investigated in this study to determine the relationship between patch size and the severity of coral bleaching. The results of the analysis of

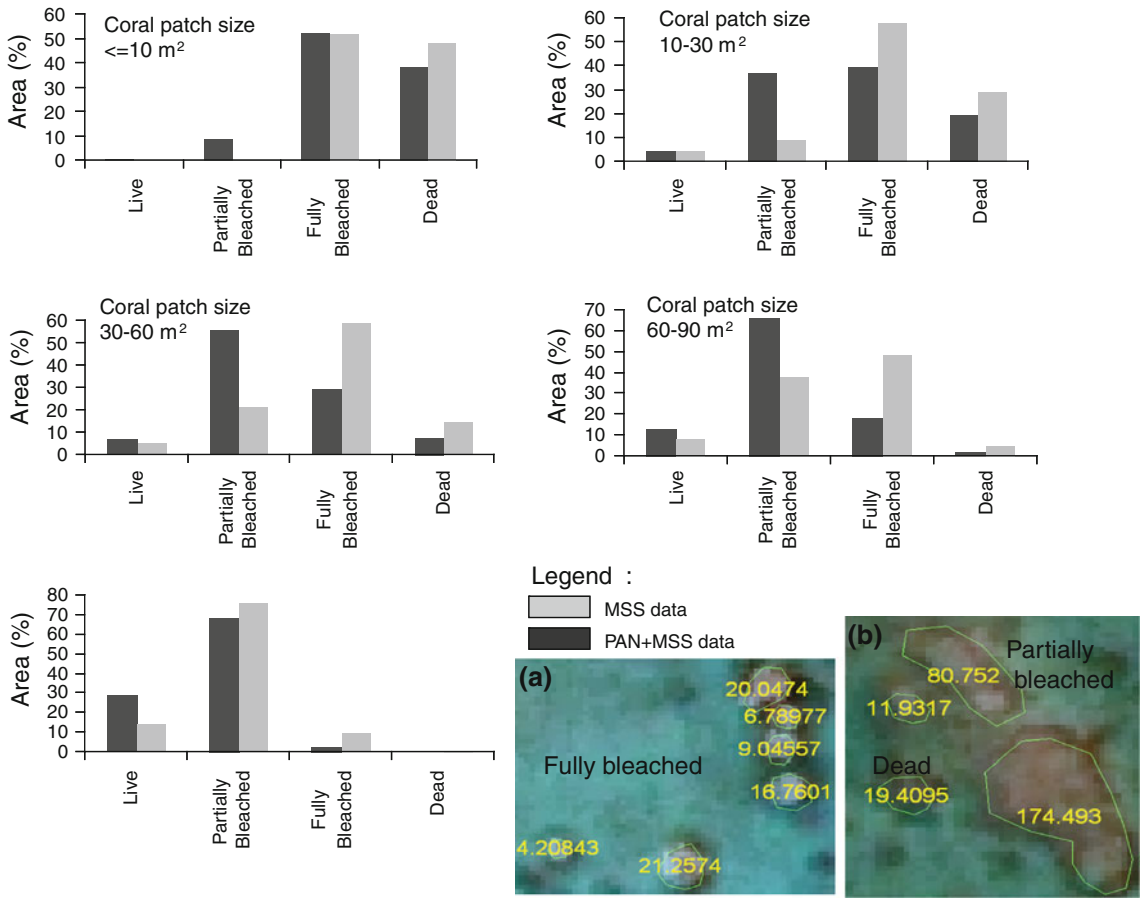

Fig. 8 Patch size distributions for coral cover in the MSS and PAN + MSS data. *Remarks*: image subsets *a* and *b* indicating the different coral patch sizes (with their respective area) delineated from the satellite image

the coral patch size distributions implied that the coral mortality and bleaching effects decreased with increasing patch size. In conclusion, future research should focus on combining these results with the information on coral species. Such a combined approach may yield more useful information about the effects of bleaching. Remotely sensed images and maps derived from high-resolution data and GIS have the potential to synoptically cover large areas of coral-reef ecosystems. Furthermore, they can detect changes in coral cover distribution and the extent of coral bleaching in relation to various factors. This approach could lead to improved local and regional management and protection of these reef resources.

Acknowledgments This work has been supported by Grant-in-Aid for Scientific Research (A) (No.17206052, No.18254003, No.20246081, No.21254002) of JSPS (The Japan Society for the Promotion of Science), Grant-in-Aid for Scientific Research on Innovative Areas (No. 20121007) of the Ministry of Education, Culture, Sports, Science and Technology (MEXT) and JST (Japan Science and Technology Agency)/JICA (Japan International Co-operation Agency) SATREPS Program, Japan. We are thankful to the two anonymous reviewers for their valuable comments and suggestions.

References

Andréfouët S, Guzman HM (2005) Coral reef distribution, status and geomorphology–biodiversity relationship in Kuna Yala (San Blas) archipelago, Caribbean Panama. Coral Reefs 24:31–42

Andréfouët S, Berklemans R, Odrizola L, Done T, Oliver J, Muller-Krager F (2002) Choosing the appropriate spatial resolution for monitoring coral bleaching events using remote sensing. Coral Reefs 21:147–154

Anselin L (2005) Exploring spatial data with GeoDa™: A workbook. Spatial Analysis Laboratory, University of Illinois, Urbana-Champaign

Brown BE (1997) Coral bleaching: causes and consequences. Coral Reefs 16:129–138

Bruno JF, Siddon CE, Witman JD, Colin PL, Toscano MA (2001) El Nino related coral bleaching in Palau, Western Caroline Islands. Coral Reefs 20:127–136

Clark CD, Mumby PJ, Chisholm JRM, Jaubert J, Andréfouët S (2000) Spectral discrimination of coral mortality states following a severe bleaching event. Int J Remote Sens 21:2321–2327

Congalton RG (1991) A review of assessing the accuracy of classification of remote sensing data. Remote Sens Environ 37:35–46

Diaz-Pulido G, McCook LJ (2002) The fate of bleached corals: patterns and dynamics of algal recruitment. Mar Ecol Prog Ser 232:115–128

Douglas AE (2003) Coral bleaching – how and why? Mar Pollut Bull 46:385–392

Elvidge CD, Dietz JB, Berkelmans R, Andréfouët S, Skirving W, Strong AE, Benjamin TT (2004) Satellite observation of Keppel Islands (Great Barrier Reef) 2002 coral bleaching using IKONOS data. Coral Reefs 23:123–132

Franklin EC, Ault JS, Smith SG, Luo J, Meester GA, Diaz GA (2003) Benthic habitat mapping in the Tortugas Region Florida. Mar Geod 26:19–34

Fujioka Y (1999) Mass destruction of the hermatypic corals during a bleaching event in Ishigaki Island, southwestern Japan. Galaxea 4:53–61

Gardner TA, Cote IM, Gill JA, Grant A, Watkinson AR (2003) Long-term region-wide declines in Caribbean coral reefs. Science 301:958–960

Goreau T, McClanahan T, Hayes R, Strong A (2000) Conservation of coral reefs after the 1998 global bleaching event. Conserv Biol 14:5–15

Hasegawa H, Ichikawa K, Kobayashi M, Kobayashi T, Hoshino M, Mezaki S (1999) The mass-bleaching of coral reefs in the Ishigaki Lagoon, 1998. Galaxea 1:31–39

Hoegh-Gulberg O (1999) Climate change, coral bleaching and the future of the world's coral reefs. Mar Freshw Res 50:839–866

Holden H, LeDrew E (1998) Spectral discrimination of healthy and non-healthy corals based on cluster analysis, principal components analysis and derivative spectroscopy. Remote Sens Environ 65:217–224

Hughes TP (1994) Catastrophes, phase shifts, and large-scale degradation of Caribbean coral reef. Science 265:1547–1551

IPCC (2007) Climate change 2007: the physical basis. In: Solomon S, Qin D, Manning M, Chen Z, Marquis M, Averyt KB, Tignor M, Miller HL (eds) Contribution of Working Group I to the Fourth Assessment Report of the Intergovernmental Panel on Climate Change. Cambridge Univ. Press, Cambridge, UK and New York, NY, p 996

Jokiel PL, Coles SL (1990) Response of Hawaiian and other Indo-Pacific reef corals to elevated temperature. Coral Reefs 8: 155–162

Kayanne H, Harii S, Yamano H, Tamura M, Ide Y, Akimoto F (1999) Changes in living coral coverage before and after the 1998 bleaching event on coral reef flats of Ishigaki Island, Ryukyu Islands. Galaxea 1:73–82

Kayanne H, Harii S, Ide Y, Akimoto F (2002) Recovery of coral populations after the 1998 bleaching on shiraho reef, in the southern Ryukyus, NW Pacific. Mar Ecol Prog Ser 239:93–103

Kleppel GS, Dodge RE, Reese CJ (1989) Changes in pigmentation associated with the bleaching of stony corals. Limnol Oceanogr 34:1331–1335

Lee A, Norman P, Wood M, Davey S (2003) Integrated sampling strategies-application at the regional and continental levels for monitoring sustainable forest management. Proceedings Joint Australia and New Zealand Institute of Forestry Conference, Queenstown, New Zealand

Loya Y, Sakai K, Yamazato K, Nakano Y, Sambali H, Van Woesik R (2001) Coral bleaching: the winners and the losers. Ecol Lett 4:122–131

Lyzenga DR (1981) Remote sensing of bottom reflectance and water attenuation parameters in shallow water using aircraft and Landsat data. Int J Remote Sens 2:71–82

Matthew MW, Adler-Golden SM, Berk A, Richtsmeier SC, Levine RY, Bernstein LS, Acharya PK, Anderson GP, Felde GW, Hoke MP, Ratkowski A, Burke HH, Kaiser RD, Miller DP (2000) Status of Atmospheric Correction Using a MODTRAN4-Based Algorithm. SPIE Proceedings, Algorithms for Multispectral, Hyperspectral, and Ultraspectral Imagery VI 4049:199–207

McClanahan TR (2004) The relationship between bleaching and mortality of common corals. Mar Biol 144:1239–1245

McWilliams JP, Cote IM, Gill JA, Sutherland WJ, Watkinson AR (2005) Accelerating impacts of temperature-induced coral bleaching in the Caribbean. Ecology 86:2055–2060

Moran P (1950) Notes on continuous stochastic phenomena. Biometrika 37:17–23

Nadaoka K, Nihei Y, Kumano R, Yokobori T, Omija T, Wakaki K (2001) A field observation on hydrodynamic and thermal environments of a fringing reef at Ishigaki Island under typhoon and normal atmospheric conditions. Coral Reefs 20:387–398

Odum EP (1963) Fundamentals of ecology. Saunders, Philadelphia, p 574

Paringit E, Nadaoka K (2003) Synergistic methods in remote sensing data analysis for tropical coastal ecosystems monitoring. Proceedings of the XXth International Society for Photogrammetry and Remote Sensing Congress, on DVD

Planck RJ, McAllister DE, McAllister AT (1988) Shiraho coral reef and the proposed new Ishigaki Island Airport, Japan. International Union for Conservation of Nature and Natural Resources, Morgas, Switzerland

Roberts E (2003) Scientists warn of coral reef damage from climate change. Marine Scientist 2:21–23

Sheppard CRC (2003) Predicted recurrences of mass coral mortality in the Indian Ocean. Nature 425:294–297

Tamura H, Nadaoka K (2005) Numerical simulation of current and thermal transport in a fringing-type coral reef. Proc 3rd Int Conf on Asian and Pacific Coasts: 659–662

Tamura H, Nadaoka K, Paringit EC (2007) Hydrodynamic characteristics of a fringing coral reef on the east coast of Ishigaki Island, southwest Japan. Coral Reefs 26:17–34

Weber AP (1993) Abandoned seas: reversing the decline of the oceans. World Watch Paper 116. World Watch Institute, Washington, p 66

Wellington GM, Glynn PW, Strong AE, Navarrete SA, Wieters E, Hubbard D (2001) Crisis on coral reefs linked to climate change. EOS Trans Am Geophys Union 82:1–6

Yamano H, Tamura M (2004) Detection limits of coral reefs bleaching by satellite remote sensing: Simulation and data analysis. Remote Sens Environ 90:86–103